SolarPACES 2023, 29th International Conference on Concentrating Solar Power, Thermal, and Chemical Energy Systems

Operations, Maintenance, and Component Reliability

https://doi.org/10.52825/solarpaces.v2i.810

Published: 20 Nov. 2024

A Maintenance Policy for Central Tower Receiver Subjected to Creep-Fatigue Damage

Huy Truong-Ba[1], Giovanni Picotti[1], Michael E. Cholette[1], Giancarlo Gentile[2], and Giampaolo Manzolini[2]

[1] Queensland University of Technology (QUT), Australia

[2] Politecnico di Milano, Italy

* Correspondence: Huy Truong-Ba, h.truongba@qut.edu.au

Abstract. This study focuses on the central receiver of solar tower plants, which is subjected to extreme heat fluxes, high temperatures, and thermal gradients leading to degradation mechanisms such as creep, fatigue, and corrosion. Although studies in literature have developed thermal models for receiver tubes to understand the damage process and estimate their lifetime, they have not addressed the uncertainty associated with receiver damage, which arises from random operating conditions and errors in creep damage predictive models. Considering the random and varying nature of damage, this paper suggests effective maintenance strategies that optimize the receiver's lifetime and minimize maintenance costs. The strategies utilize a simulation-optimization approach and incorporate uncertain operating conditions and creep-fatigue models. The illustration case study shows that the proposed maintenance strategy can reduce the maintenance cost up to 37% versus the interval replacement of all panels.

Keywords: Receiver Damage, Receiver Maintenance, Central Tower Receiver, Operation & Maintenance for CSP Plants, Predictions Uncertainty

1. Introduction

The central receiver is a crucial component of a solar tower plant, enduring extreme heat fluxes, high temperatures, and thermal gradients that accelerate degradation mechanisms such as creep, fatigue, and corrosion. Degradation is primarily driven by the tube temperature distribution, and previous studies have focused on developing detailed thermal models for the receiver tubes [1], [2]. Thus, the proper understanding of the damage process and accurate estimations for the lifetime of receivers in solar tower plants are paramount to operate the receiver efficiently and to develop effective maintenance plans for receivers.

Gentile et al. [3] developed a methodology to determine the damage due to creep and fatigue for receiver tubes that therefore enables to estimate the lifetime of the receiver. According to the results presented in their study creep is the primary factor leading to receiver degradation. Moreover, predicting creep damage and lifetime involves fitting experimental data to predefined mathematical models like Larson-Miller [4] or Wilshire equations [5]. However, the work of Gentile et al. [3] does not address the uncertainty of the receiver's damage, which originates from the random operating conditions of the receiver (e.g. due to oscillating values

of DNI). In addition, the creep models' predictions are prone to errors that further enhance uncertainty in the damage and lifetime estimation of the receiver [6].

Since the damage caused by creep and fatigue exhibits significant randomness and varies among receiver panels, maintenance planners should consider this uncertainty while developing an effective maintenance plan that balances the damage among the receiver's panels. This work proposes a novel maintenance strategy that extends the lifetime of the central tower receiver while minimizing maintenance costs. The strategy is optimized using a simulation-optimization approach and is based on a creep-fatigue damage model of receiver tubes, which considers both uncertain sources of receiver operating conditions and creep-fatigue models.

2. Damage distribution determination

The failure of a receiver panel happens when its cumulative normalized damage reaches 1. The creep-fatigue damage depends on the flux distribution on the panel and, given a constant aiming strategy, random fluctuations of DNI. Thus, the daily damage of receiver panels is not a fixed value but a random variable and follows some statistical distribution.

Another source of uncertainty in the damage determination is the accuracy of the models exploited for creep damage assessment. A previous study by the authors [6] has discussed the errors induced by creep models and statistical methods to quantify them. It has been shown that errors depend on the material, size of experiment data and adopted (creep) models. Therefore, for proper estimation of receiver panels lifetime, the distribution of damages should be identified, and they should include both the randomness caused by DNI and the uncertainty of damage models.

2.1 Determination of empirical damage distribution via simulation approach

This section presents the approach for determining the distribution of tubes' damage considering the random DNI and uncertainty of creep-fatigue models. The receiver operation follows a cycle throughout the day that follows the variation of DNI values between sunrise and sunset. Therefore, the normalized damage of one cycle, composed by fatigue and creep damages, is equivalent to one-day damage. The general approach for building the damage distribution is via a Monte-Carlo simulation: A sample of random DNI is sampled from historical data of DNI. For each sample, the Creep-Fatigue Analysis model is applied to compute the related damage. Therefore, all damage values for the DNI sample are determined and the statistics of damages are determined.

The main drawback of the aforementioned method is related to its long computational time, mostly due to running multiple instances of the computationally expensive Creep-Fatigue model. Moreover, using this approach, all DNI profiles for each time period (e.g. month) should be considered to run the required simulations to obtain the appropriate damage statistics for a whole year. An approximate method is explored to overcome such limitations. This method is also based on the same procedure and simulation, but it consists of 2 stages (Figure 1):

- For the 1st stage, a set of prototypical DNI is selected from historical (random) DNI. Then the creep-fatigue calculation model is applied for this set of DNI, and therefore, the representative damages (for all prototypical DNI profiles) are determined.

- For the 2nd stage, a Monte-Carlo simulation is conducted to identify the damage distribution. For each sampled DNI, the similarity of this DNI and prototypical DNI is

calculated as weights. These weights are then used to compute the damage of the sampled DNI. After running simulation for 10,000 repetitions for each month, the damage statistics of each month are identified.

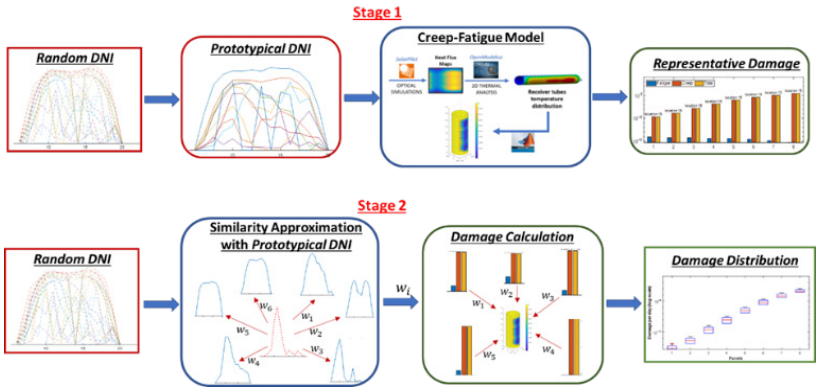

Figure 1. *Approximation Approach for Creep-Fatigue damage distribution determination*

2.2 Modifying damage calculation to include the error of model

The damage computation model above is developed starting from the model described in [3], which is modified to include the computational errors that are represented with a noise distribution. As demonstrated in [3], the damage caused by fatigue is negligible compared to that caused by creep, especially for the typical materials used for CSP receivers. Hence, in this study, the uncertainty associated with the fatigue model is ignored, but the calculation of damage caused by fatigue is still presented.

In a recently published study [6] the authors discussed the errors of creep models for some potential materials used for manufacturing tubes inside receiver panels. The creep estimation methods considered in this work are Larson-Miller (LMP) [4] and Wilshire Equation (WE) with two approaches: single region [7] and region splitting [8]. The statistical method of bootstrapping was used to analyze and determine the distributions of the errors. Figure 2 shows the error distributions of the three methods in term of rupture time (i.e. lifetime) of IN740H. The numbers under the boxplots indicate the numbers of experiment data points within each rupture time range. It can be seen that different methods yield different error distributions for separate ranges of rupture time. For the IN740H, the LMP method provides unbiased and narrow error distributions, particularly for the range of long rupture time which is the zone for receiver operations. Thus, in this study the LMP model is used for calculation of creep damage for the receiver with material IN740H. The damage for day i is computed as:

$$D_{panel}(DNI_i) = D_{panel}^{creep}(DNI_i) + D_{panel}^{fatigue}(DNI_i) \quad (1)$$

where $DNI_i = \left(DNI_{i,h} \middle| h = 0, \dots, 23\right)$ is the hourly DNI profile, $D_{panel}^{creep}(DNI_i)$ and $D_{panel}^{fatigue}(DNI_i)$ are the daily damage caused by creep and fatigue, respectively. Among them the $D_{panel}^{creep}(DNI_i)$ is stochastic due to the randomness associated with the selected creep model:

$$D_{panel}^{creep}(DNI_i) = \sum_{h=0}^{23} \frac{dt_h}{t_{rupture,h}} \quad (2)$$

where $$t_{rupture,i} = (\epsilon + 1) \cdot G_{creep}(DNI, \text{aiming strategy}, \text{material}) \quad (3)$$

where $G_{creep}(.)$ represents the creep model and the error ratio of the model $\epsilon = (Actual - Estimate)/Estimate$ is assumed to follow a Normal distribution, $\epsilon \sim \mathcal{N}(\mu_\epsilon, \sigma_\epsilon)$ (truncated below -1). From the work [6], the parameters $\mu_\epsilon, \sigma_\epsilon$ are set at 0.03 and 0.4, respectively.

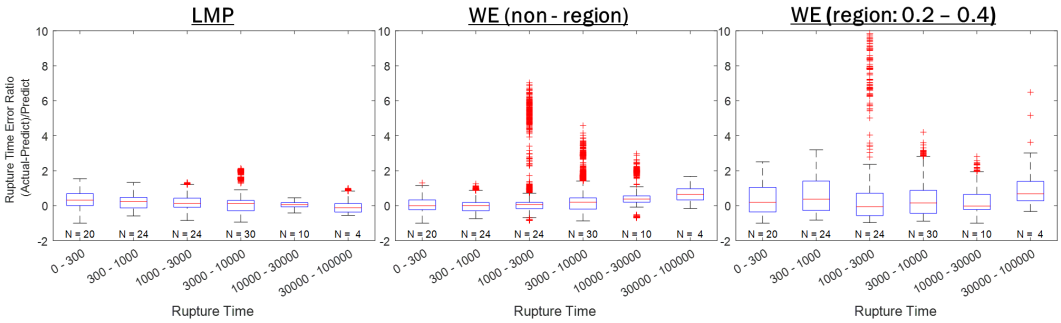

Figure 2. *IN740H - Prediction Errors with respect to Length of Rupture Time (h) [6]*

2.3 Uneven damage distribution in external cylindrical receivers

The daily damage of external cylindrical receivers varies along the year and its not equally distributed among the different panels. An example of typical damage distribution for the panels of a cylindrical receiver located in Mount Isa (Australia) in January and July are presented in Figure 3. The fatigue damage is higher at panel 1 (facing South) in summer (January), but it is higher at panel 8 in winter (July). The creep damage is the dominant damage for the analyzed receiver, and it is highest at panel 8. Considering seasonal effects, the fatigue damage in summer is subjected to larger variations as shown in Figure 3 by the wider damage distribution for January (summer in the Southern hemisphere). This is due to a higher stability in terms of DNI during winter (dry season in Mount Isa), opposed to the higher fluctuations of DNI experienced in summer (rainy season) due to frequent rain events. Moreover, it is interesting to observe that the damage experienced during winter is higher than summer regardless of the average lower values of DNI. The reason behind this is related to the HTF mass flow rate ($\dot{m}_{htf}$) control in the receiver: lower values of DNI during winter induces a lower $\dot{m}_{htf}$ inside the receiver tubes which originates higher metal temperature of tubes and hence more severe creep damage.

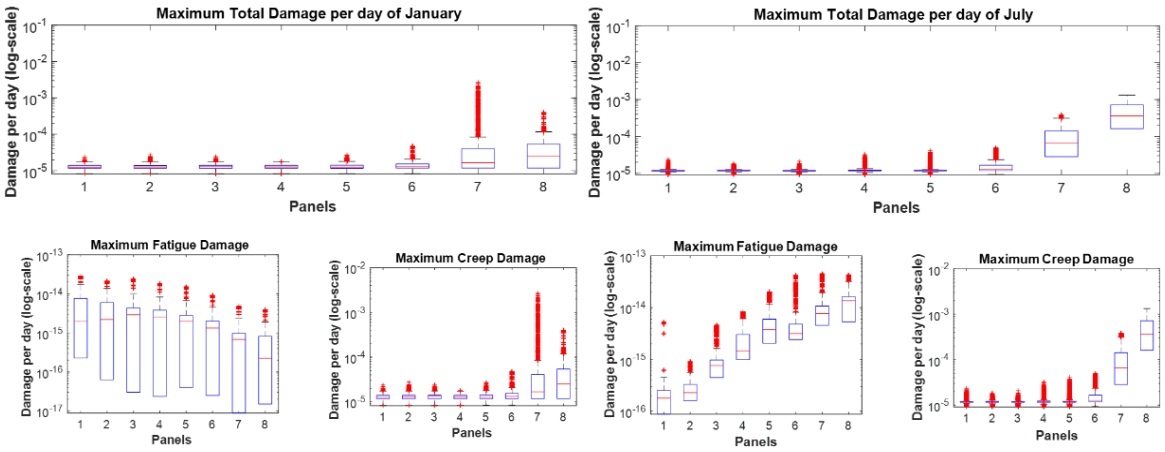

Figure 3. *Daily Damages Distribution*

3. Maintenance strategies

The figure above suggests that varying damage across receiver panels may be exploited to balance the accumulated damage by swapping/relocating panels at some planned times. A possible maintenance strategy along these lines is briefly described as follows: at a specific time t_k chosen for preventive maintenance, the tower receiver is shutdown, and all panels $i, i = 1,2, \dots, N_{pan}$ are disassembled. In the stage 1 of maintenance procedure, a number of the most damaged panels are replaced and the new and remaining panels are ranked by their damage levels, denoted by $r_i, i = 1..N_{pan}$, $r_i \in \{1,2, \dots, N_{pan}\}$ and r_i may be different to i. Subsequently in the stage 2, these panels are assigned to the new locations in the receiver tower according to their ranks, the panel with highest damage rank will be assembled to the lowest damage location, the 2nd rank one will go to the 2nd lowest damage location and so on. Thus, the aim of the maintenance optimization model is to determine the best time for maintenance and the number of panels to be replaced. The maintenance plan is developed and optimized for a finite horizon that is usually the proposed lifetime of whole CSP plant. The optimization model of maintenance strategy is to minimize the total cost of the whole planning horizon. An illustration of the maintenance strategy is presented in Figure 4 with 8 panels.

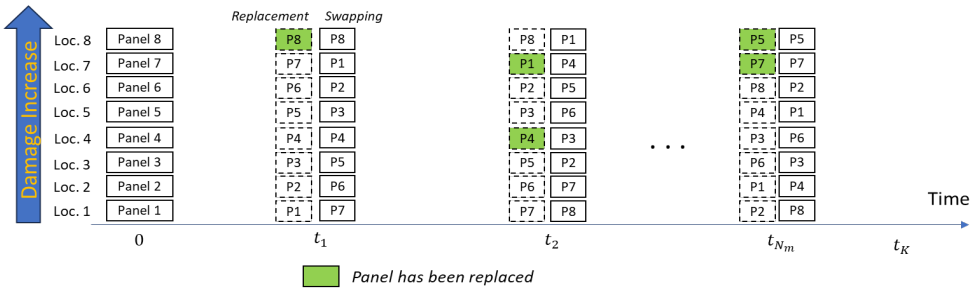

Figure 4. *Illustration of maintenance strategy with 8 panels*

3.1 Cost model

A cost model is defined to provide inputs to the optimization of the proposed maintenance strategy, including maintenance actions, replacements, and failure costs based on labor, production loss (or downtime), and material or panel costs. The cost components of failure cost and maintenance cost defined in Eq. (4) and Eq. (5) depend on CSP plants characteristics and unfortunately, the authors currently cannot access the real data of an operating receiver. Thus, in this study, the cost components are obtained with reasonable assumptions and previous knowledge. However, this does not affect the contribution of the study and the significance of the performed analysis. The failure cost is defined as follows:

$$c_{fail} = c_{hazard} + c_{panel} + c_{replace} + c_{loss} \cdot d_{fail} \quad (4)$$

where c_{hazard} is the hazard cost due to a broken panel tube, c_{panel} is the cost of a panel, $c_{replace}$ is the service cost for replacement, c_{loss} is the average cost rate ($/day) for generation losses during the receiver shutdown, d_{fail} is the average duration of shutdown due to failure.

For a maintenance event occurring at an arbitrary maintenance time t_k, two actions are involved: replacing a number of panels $N_{rep,k}$ and changing the locations of the remaining panels $N_{rot,k}$. Hence, the maintenance cost is defined as follows:

$$c_{maint,k}(N_{rep,k}, N_{rot,k}) = (c_{panel} + c_{replace}) \cdot N_{rep,k} + c_{rot} \cdot N_{rot,k} + c_{loss} \cdot d_{maint,k} \quad (5)$$

where c_{rot} is the unit service cost of swapping a pair of panels and d_{maint} is the duration of planned shutdown for maintenance activities.

3.2 Maintenance strategies and optimization

In this study, the maintenance strategies will be optimized according to a Simulation – Optimization approach. Denote $t_k, k = 1,2,\dots,K$ as the potential times for doing maintenance (e.g. k are indices of years in which maintenance may occur), and t_K as the end time of horizon. Let $x_k \in \{0,1\}$ be the decision variable of doing maintenance at time t_k or not, and $\mathcal{M}$ be the set of maintenance time indices, $\mathcal{M} = \{k | x_k = 1, k = 1,2,\dots,K\}$.

Let $N_{rep,k}, k \in \mathcal{M}$ be the number of replaced panels at maintenance time t_k, and $\mathcal{N} = \{N_{rep,k} | k \in \mathcal{M}\}$ be the set of all $N_{rep,k}$. The variable $N_{rep,k}$ also need to be optimized in the optimization model. We also denote $N_{rot,k}, k \in \mathcal{M}$ as the number of panel swaps at maintenance time t_k. The number of swaps $N_{rot,k}$ depends on the ranking of simulated damages as described above. The optimization model is then defined as follows to minimize the total cost TC:

$$\begin{aligned} \min_{\mathcal{M},\mathcal{N}} TC(\mathcal{M},\mathcal{N}) &= C_{fail}(\mathcal{M},\mathcal{N}) + C_{maint}(\mathcal{M},\mathcal{N}) \\ &= \sum_{k \in M} \rho^k \left[c_{maint,k}\left(N_{rep,k}, N_{rot,k}\right) + c_{fail} \cdot \mathbb{E}\{N_{fail,k}(\mathcal{M},\mathcal{N})\} \right] \end{aligned} \quad (6)$$

Subject to: $0 \le N_{rep,k} \le N_{pan} \quad \forall k \in \mathcal{M}$

All panel are relocated at every $k \in \mathcal{M}$

where ρ is the discount factor, and N_{fail} is the random variable of number of failures.

For solving the optimization model above, the Simulation – Optimization approach is used with GA method built in MATLAB (Figure 5). The decision variables $\mathcal{M}, \mathcal{N}$ are translated to GA integer variables and the fitness function is calculated via simulation based on the damage distributions described in Section 2.

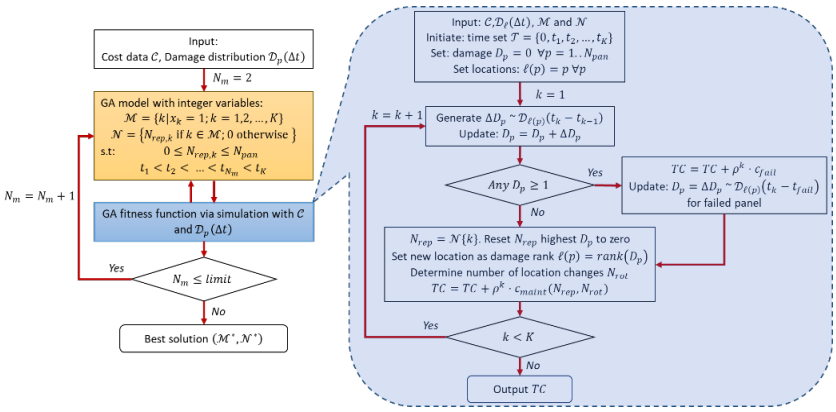

Figure 5. *Simulation – Optimization approach*

3.3 Alternative Simplified Maintenance Strategies

The proposed maintenance strategy above is benchmarked with its two simplified versions:

1. Panels are not rotated and their location is fixed until replacement or failure occur. Thus, a replacement decision for each panel is assessed at each maintenance event.

$$\min_{\mathcal{M},\mathcal{N}} TC = \sum_{k\in\mathcal{M}} \rho^k \left[c_{rep} \cdot N_{rep,k} + c_{loss} \cdot d_{maint,k} + c_{fail} \cdot \mathbb{E}\{N_{fail,k}(\mathcal{M},\mathcal{N})\}\right] \quad (7)$$

Subject to: $0 \le N_{rep,k} \le N_{pan} \ \forall k \in \mathcal{M}$

2. The panel replacement is conducted for all panels, regardless of their damage state. Panels may be swapped and their location changed during maintenance, until a replacement decision is made and all of them are replaced simultaneously.

$$\min_{\mathcal{M},\mathcal{N}} TC = \sum_{k\in\mathcal{M}} \rho^k \left[c_{rep} \cdot N_{rep,k} + c_{rot} \cdot N_{rot,k} + c_{loss} \cdot d_{maint,k} + c_{fail} \cdot \mathbb{E}\{N_{fail,k}(\mathcal{M},\mathcal{N})\}\right] \quad (8)$$

Subject to: $N_{rep,k} = \{0, N_{pan}\} \ \forall k \in \mathcal{M}$

4. Case Study

A case study for a hypothetical receiver tower of a 100MW CSP plant located in the Australian outback, close to the town of Mount Isa in North Queensland. The receiver is made of 16 panels, 8 for each path through which flows the Heat Transfer Fluid (HTF). In this case study the analysis is conducted for one path only (East side), corresponding to a half of the receiver (i.e. 8 panels), assuming that the receiver behaves symmetrically. In the thermal and creep-fatigue models each panel is represented by one tube that is divided into 20 longitude portions for calculation purposes. The methodology developed for this case study can be applied on both sides of the receiver. The assumed costs used in this case study are reported in Table 1. The time horizon of the CSP plant is assumed to be 70 years and discount factor $\rho = 0.99$ for illustrative purpose.

Table 1. *Cost Assumptions*

Quantities	Values	Quantities	Values
$\boldsymbol{d_{fail}}$	$70\ days$	d_{maint}	$7\ days$
$\boldsymbol{c_{pan}}$	$\$197{,}000/pan$	c_{rot}	$\$20{,}000/swap$
$\boldsymbol{c_{replace}}$	$\$10{,}000/pan$	c_{loss}	$\$120{,}000/day$

The optimized maintenance plans, i.e. proposed strategy (PS), no swapping panels strategy (NoSS), and replacing all panels together (RAS), are shown in Figure 6 below. It is noted that due to the symmetry of tower receivers, the strategies presented here are developed for one half of the receiver only (i.e. 8 panels). The other side of the receiver is assumed to be subjected to similar damage and maintained following the same strategy.

The intervals among maintenance events are almost equal across all strategies. The RAS strategy results in one more maintenance event with respect to the other two strategies, and it incurs the greatest number of replacements (represented by the green panels in Figure 6). The NoSS strategy provides the same number and timing of maintenance events as the proposed maintenance strategy (PS) but yields two more panel replacements.

Figure 7 provides the distributions of maximum (normalized) damage values of all panels during operating horizon (i.e. 70 years) for each strategy. These distributions show that the PS strategy yields the similar maximum damage to NoSS strategy, and it is just a little higher than the RAS strategy. It indicates the advantage of the proposed maintenance strategy in reducing the number of panel replacements while still maintaining the failure risk of receiver.

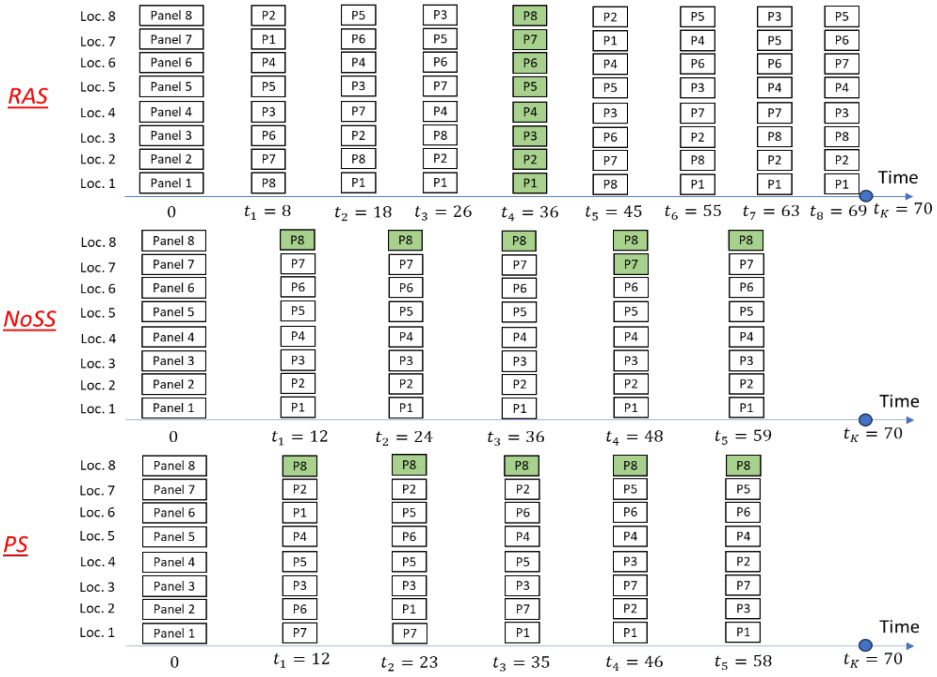

Figure 6. *Maintenance strategies*

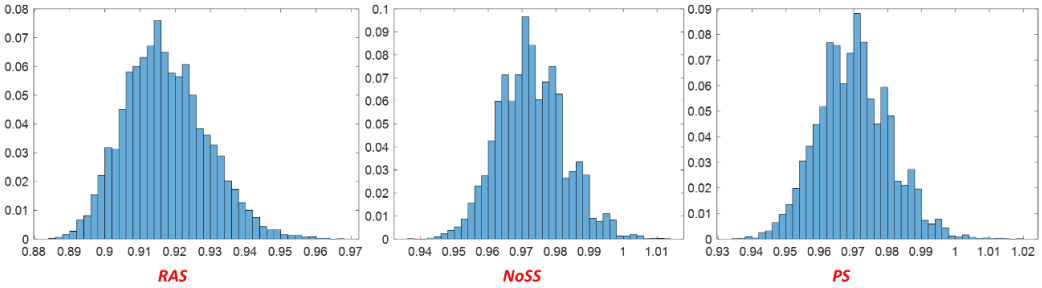

Figure 7. *Distributions of maximum damage*

Figure 8 below shows the cost components of each individual maintenance strategy. The maintenance policy in which all panels must be replaced together (RAS) has the highest cost (i.e. 86% higher than PS), which is mostly due to panel replacements. It indicates that many panel replacements in this maintenance strategy are too early. For the proposed strategy (PS) and the maintenance policy without panel rotation (NoSS), the downtime cost for maintenance is the dominant cost category. The NoSS maintenance strategy can save the panel swapping cost, and its total cost is a little lower (i.e. 4.8%) than PS with both swapping and replacement because it also has a higher number of replacements versus PS. It is worth noting that if the swapping cost is lower, and the replacement cost is higher, the PS strategy may be a preferable option for maintenance of tower receivers.

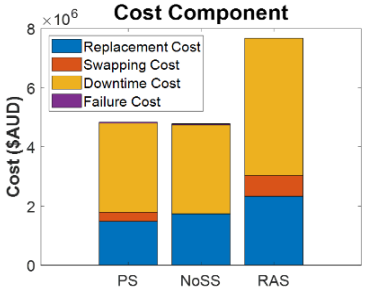

	PS	NoSS	RAS
N_{rep}	5	6	8
N_{rot}	15	0	19
N_{fail}	0.0042	0.0055	0

Figure 8. *Numbers of replacements, rotations, and costs of maintenance strategies*

5. Conclusion

This paper presents and discusses a potential maintenance activity for CSP central tower receivers where their panels can be replaced and relocated depending on their damage state. Two subsequent simpler strategies were also investigated for comparison. All the proposed maintenance strategies have been optimized via a simulation and optimization approach, in which the simulation is based on the dominant creep damage whose occurrence has a random component. The latter is originated by the operating conditions of the receiver, subjected to continuously varying external conditions (e.g., DNI), and the inherent uncertainties of predictive creep models. The results of the performed analysis show that the proposed maintenance strategies can extend the expected lifetime of central receivers and reduce O&M costs of solar tower plants up to 37% compared with the receiver replacement.

For future work, we focused on developing condition-based or digital-twin based maintenance policy for receivers, in which the conditions and operating status of receivers are monitored via inspection and physical-digital models and therefore, the failures can be predicted in advance and inform subsequent maintenance/repair decisions.

Author contributions

Huy Truong-Ba: Conceptualization, Software, Formal analysis, Investigation, Methodology, Validation, Writing-original draft.

Giovanni Picotti: Software, Writing-review & editing.

Michael E. Cholette: Conceptualization, Methodology, Supervision, Writing-review & editing.

Giancarlo Gentile: Software, Methodology, Writing-review & editing.

Giampaolo Manzolini: Writing-review & editing.

Competing interests

The authors declare that they have no competing interests.

Data availability statement

The data used in this study includes DNI and cost information. DNI is the historical data from Bureau of Meteorology of Queensland – Australia. The cost information has been made up from System Advisory Model (SAM) [9].

References

[1] G. Picotti *et al.*, “Object-oriented modelling of an external receiver for solar tower application: Dynamic simulation and impact of soiling,” in *AIP Conference Proceedings*, AIP Publishing LLC, 2020, p. 160003.

[2] W. R. Logie, J. D. Pye, and J. Coventry, “Thermoelastic stress in concentrating solar receiver tubes: A retrospect on stress analysis methodology, and comparison of salt and sodium,” *Solar Energy*, vol. 160, pp. 368–379, 2018, doi: https://doi.org/10.1016/j.solener.2017.12.003.

[3] G. Gentile, G. Picotti, M. Binotti, M. E. Cholette, and G. Manzolini, “Dynamic thermal analysis and creep-fatigue lifetime assessment of solar tower external receivers,” *Solar*

Energy, vol. 247, pp. 408–431, Nov. 2022, doi: 10.1016/j.solener.2022.10.010.

[4] F. R. Larson and J. Miller, “A Time-Temperature Relationship for Rupture and Creep Stresses,” *Journal of Fluids Engineering*, vol. 74, no. 5, pp. 765–771, Jul. 1952, doi: 10.1115/1.4015909.

[5] B. Wilshire and A. J. Battenbough, “Creep and creep fracture of polycrystalline copper,” *Materials Science and Engineering: A*, vol. 443, no. 1, pp. 156–166, Jan. 2007, doi: 10.1016/j.msea.2006.08.094.

[6] V. Gray, H. Truong-Ba, G. Picotti, and M. E. Cholette, “Using statistical analysis to understand creep modelling error and the ramifications for Solar Tower receivers,” *Solar Energy Materials and Solar Cells*, vol. 257, p. 112408, Aug. 2023, doi: 10.1016/j.solmat.2023.112408.

[7] B. Wilshire and P. J. Scharning, “A new methodology for analysis of creep and creep fracture data for 9–12% chromium steels,” *International Materials Reviews*, vol. 53, no. 2, pp. 91–104, Mar. 2008, doi: 10.1179/174328008X254349.

[8] M. Whittaker, W. Harrison, C. Deen, C. Rae, and S. Williams, “Creep Deformation by Dislocation Movement in Waspaloy,” *Materials*, vol. 10, no. 1, p. 61, Jan. 2017, doi: 10.3390/ma10010061.

[9] P. Gilman, N. Blair, M. Mehos, C. Christensen, S. Janzou, and C. Cameron, “Solar Advisor Model: User Guide for Version 2.0,” no. August, p. 133, 2008.